OPal
Open Palaeontology

Reconstruction of CO_2 levels in the Late Devonian - Mississippian on the basis of decoupling of C-isotope composition of conodont elements and host carbonates

Andrey V. Zhuravlev[a,1]

The study explores a novel proxy for reconstructing atmospheric CO_2 concentrations during the Late Devonian–Mississippian, a key interval marked by the transition from a greenhouse to an icehouse climate and the onset of the Late Palaeozoic Ice Age. Traditional proxies for Palaeozoic CO_2 levels, such as palaeosols and vascular plant and phytoplankton remains, are limited by scarcity, poor dating, or susceptibility to diagenetic alteration. To address these challenges, this work evaluates the decoupled carbon isotope composition of conodont elements and host carbonates. Based on integrated isotope analyses and comparison with compiled CO_2 estimates, the study reveals a significant negative correlation between the decoupling of carbon isotope composition of conodont elements and host carbonates and atmospheric CO_2 content. The results indicate taxon-specific trends, with Ozarkodinida and Prioniodinida exhibiting similar regression gradients but distinct intercepts, suggesting ecological or physiological influences on isotopic fractionation. The findings support the potential of the decoupling of carbon isotope composition of conodont elements and host carbonates as a potential proxy for atmospheric CO_2, with implications for reconstructing spatial and temporal variations in Palaeozoic carbon cycle and climate dynamics.

Introduction

Atmospheric carbon dioxide concentration is a key driver of climate change and biosphere perturbations (Foote, 1856; McKenzie and Jiang, 2019; Percival *et al.*, 2024). However, it is difficult to find reliable and abundant proxies for the CO_2 concentration in deep time, so the Palaeozoic variations of this parameter are mainly derived from computer models (e.g. COPSE, GEOCARB, GEOCARB_NET, GEOCLIM, GEOCARBSULFvolc) (Berner, 1994; Berner and Kothavala, 2001; Lenton *et al.*, 2018; Mills *et al.*, 2019; Goddéris *et al.*, 2014; Royer *et al.*, 2014; Marcilly *et al.*, 2021; Torsvik *et al.*, 2024) and do not take into account local and regional variations in CO_2 concentrations.

Some methods are linked to the study of palaeosols and vascular plant remains (Beerling *et al.*, 1998; Royer, 2001; Breecker *et al.*, 2010), which are not common in the Palaeozoic fossil record and are usually poorly dated. In marine deposits, the carbon isotopic composition of organic matter can be used to estimate CO_2 concentration, with some assumptions (Freeman and Hayes, 1992; Hayes *et al.*, 1999; Pagani *et al.*, 1999a, 1999b; Witkowski *et al.*, 2018). In this case, the CO_2 signal may be lost by primary and secondary factors, including the variations in bioproductivity and in the vital effect among different types of phytoplankton, secondary changes in rock and organic matter composition during diagenesis. The aim is to develop a method for reconstructing atmospheric CO_2 content in the atmosphere ($p$$CO_2$ [atm]) during the Late Devonian-Mississippian based on data from marine sedimentary records.

The Late Devonian-Mississippian was a time of climatic changes that resulted in a transition from a greenhouse climate to an icehouse climate and the onset of the Late Palaeozoic Ice Age (Fielding *et al.*, 2008). Decreasing atmospheric CO_2 levels are thought to be a major driver of these climatic perturbations

(Montañez and Poulsen, 2013). Nevertheless, data on CO_2 levels in the Late Devonian-Mississippian interval are scarce (Foster *et al.*, 2017). The main sources of these data are the carbon isotopic composition of pedogenic carbonates (Muchez *et al.*, 1993; Mora *et al.*, 1996; Ekart *et al.*, 1999; Foster *et al.*, 2017) and phytoplankton phytane (Witkowski *et al.*, 2018). Elevated CO_2 concentrations serve to drive or amplify high global temperatures as a result of the greenhouse effect, whereas the reduced CO_2 levels contribute to maintaining low global temperatures (Berner and Kothavala, 2001; Crowley and Berner, 2001; Royer *et al.*, 2004; Came *et al.*, 2007). Global temperature and palaeolatitude exert control over the O-isotope composition of marine biogenic carbonates ($\delta^{18}C_{carb}$), with local water temperature acting as a moderating factor (Veizer and Prokoph, 2015; Grossman and Joachimski, 2022). Besides the global temperature, CO_2 concentrations affect the primary bioproductivity of terrestrial and aquatic ecosystems and the intensity of weathering. Both bioproductivity and weathering drive the C-isotope composition of biogenic carbonates ($\delta^{13}C_{carb}$). Therefore, some correlation between $\delta^{13}C_{carb}$ and atmospheric CO_2 is expected (e.g. Wolf-Gladrow *et al.*, 1999).

In scenarios where atmospheric CO_2 is abundant, the partial pressure of CO_2 in seawater ($p$$CO_2$ [sw]) increases, thereby increasing the availability of dissolved inorganic carbon (DIC) to

[1]To whom correspondence should be addressed: micropalaeontology@gmail.com

phytoplankton. This leads to less isotopic discrimination against ^{13}C and results in higher $\delta^{13}C$ values of phytoplankton. At the same time C-isotope fractionation by phytoplankton increases with increasing of pCO_2 [sw] (Hartke et al., 2021). Conversely, when pCO_2 [atm] is low, pCO_2 [sw] decreases, reducing the concentration of DIC available for photosynthesis (Wolf-Gladrow et al., 1999). Phytoplankton must then discriminate more strongly against ^{13}C to meet their carbon needs, resulting in lower $\delta^{13}C$ values of phytoplankton (Hartke et al., 2021). However, C-isotope fractionation by phytoplankton decreases with decreasing pCO_2 [sw] (Hartke et al., 2021). Overall, the C-isotope composition of phytoplankton depends on the C-isotope composition of DIC, which is the main source of carbon for phytoplankton. In turn, $\delta^{13}C$ values of DIC are controlled by temperature: the higher the temperature is, the smaller the difference is between $\delta^{13}C$ value of atmospheric CO_2 and the $\delta^{13}C$ value of DIC (Yoshioka, 1997).

The stable carbon isotope composition ($\delta^{13}C$) of modern phytoplankton exhibits a complex relationship with environmental factors including CO_2 concentration, taxonomic affiliation, cellular morphology (size and form), and growth rate. These parameters collectively influence the degree of carbon isotope fractionation occurring during CO_2 assimilation by phytoplankton, resulting in variations in $\delta^{13}C$ values in organic matter relative to aqueous CO_2 (Popp et al., 1999; Hayes et al., 1999; Hartke et al., 2021). Notably, the relationship between carbon isotope fractionation and CO_2 content is not universally consistent; while positive correlations have been documented in upwelling zones, negative correlations are observed in subantarctic and equatorial oceanic regions (Popp et al., 1999; Hayes et al., 1999). The magnitude of this fractionation, often quantified as the difference in $\delta^{13}C$ values between phytoplankton organic matter and carbonates (DELTA C), provides a proxy for past CO_2 conditions (Hayes et al., 1999; Hartke et al., 2021). Importantly, DELTA C is independent of the isotopic signature of atmospheric CO_2, unlike the $\delta^{13}C$ values of organic matter and carbonates (Hayes et al., 1999, fig. 5).

Thus, the effects of CO_2 concentration on phytoplankton C-isotope composition may be very different. In addition, taphonomic processes may affect the $\delta^{13}C$ values of phytoplankton due to the instability of organic matter in the sedimentary record.

Another possible proxy for atmospheric CO_2 concentration is the C-isotope composition of conodont elements ($\delta^{13}C_{con}$). Conodonts were first-level consumers (Balter et al., 2019; Zhuravlev, 2020); hence, the C-isotope composition of conodont elements reflects the isotope composition of some phytoplankton species consumed by conodonts, and a vital effect inherent to a conodont animal. $\delta^{13}C_{con}$ and $\delta^{13}C_{org}$ of bulk organic matter values show a weak positive correlation (R = 0.497, n = 11, p = 0.12; Kotik et al., 2021). The difference between $\delta^{13}C_{con}$ and $\delta^{13}C_{org}$ values varies from about 1 ‰ to almost 5 ‰, which can be interpreted as a consequence of changes in the trophic web or/and the intensity of diagenetic processes. The C-isotope composition of phytoplankton is controlled by pCO_2 [sw], which is linked to pCO_2 [atm], water temperature and salinity according to Henry's Law (Witkowski et al., 2018; Hartke et al., 2021). The vital effect inherent to a conodont animal was probably controlled by taxonomy-related physiological peculiarities.

Considering the high resistance of the C-isotope signal of conodont elements in diagenetic processes (Zhuravlev, 2023), the C-isotope composition of conodont elements seems more promising as an atmospheric CO_2 proxy for the Late Devonian-Mississippian interval, which is characterised by abundant and diverse conodonts.

Materials and methods

This study uses the results of the compilation of pCO_2 [atm] provided by Foster et al. (2017), alongside the author's conodont data. To mitigate for high frequency temporal variability of CO_2 concentration, mean values are used for each conodont zone, calculated from the most probable CO_2 content values provided by Foster et al. (2017). The age model used to relate conodont data to the pCO_2 [atm] values follows Haq and Schutter (2008, supporting online material). The pCO_2 [atm] standard deviation ranges from 0.4 in the latest Viséan (*Lochriea nodosa* Zone) to 54.7 in the latest Famennian (*Siphonodella (Eos.) sulcata* Zone) Table 1.

Preparation of samples for the conodont study followed standard methods (Harris and Sweet, 1989). The conodont elements extracted from the host rock were washed with ethanol and distilled water, then analyzed for carbon isotope values using a DELTA V Advantage mass spectrometer equipped with a Thermo Electron Continuous Flow Interface (ConFlo III) and Element Analyzer (Flash EA 1112). The conodont elements were placed in a tin capsule and fed into the Element Analyzer. The mass spectrometer analysed CO_2 gas resulting from high temperature (approximately 900 °C) combustion. International standard USGS-40 (L-Glutamic acid) was used. The precision of the $\delta^{13}C_{con}$ value is ±0.15 ‰, and measured values are reported relative to the VPDB (Vienna Pee Dee Belemnite) standard. The conodont elements contain both organic and inorganic carbon, with a mean difference in $\delta^{13}C$ values of about 0.2 ‰. The observed difference between $\delta^{13}C$ values of different conodont tissues ranges from 0.2 ‰ up to 1.6 ‰ (Zhuravlev, 2023). Thus, the analyses of bulk conodont elements provide integrated $\delta^{13}C_{con}$ values.

The host carbonates from the same samples were studied with respect to carbonate carbon isotopes composition. The carbonate powder for isotope analysis was extracted from fresh surfaces of rock samples with a steel microdrill, mainly from the micritic or fine-bioclastic matrix. The carbon isotope composition of the carbonates was studied using a DELTA V Advantage mass spectrometer with sample preparation on a Gas Bench II line following standard methods. $\delta^{13}C_{carb}$ values were reported relative to the VPDB
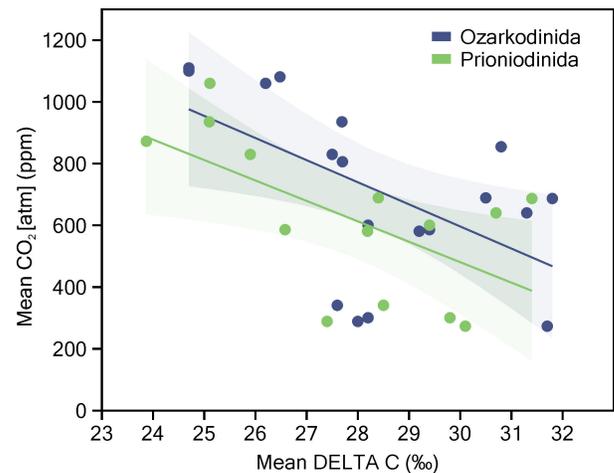

Figure 1. Bivariate plot of mean decoupled C-isotope composition of conodont elements and host carbonates (DELTA C) versus mean atmospheric CO_2 concentration (mean CO_2 [atm]) for two conodont orders-Prioniodinida (green circles) and Ozarkodinida (blue circles). The coloured areas represent 95 % confidence bands for the ordinary least squares regression lines.

Table 1. Data used in this study (Foster *et al.*, 2017; Zhuravlev, 2023 with additions).

Order	Stage	Conodont Zone	N	$\delta^{13}C_{carb}$ VPDB (‰)	$\delta^{13}C_{con}$ VPDB (‰)	DELTA C (‰)	DELTA C Std Dev	Mean CO$_2$ (ppm)	Mean CO$_2$ Std Dev
Priniodinida	Serpukhovian	*G. bollandensis*	2	0.6	-27.9	28.5	0.47	340.9	16.9
Priniodinida	Serpukhovian	*L. ziegleri*	6	1.4	-26.0	27.4	2.10	288.8	14.3
Priniodinida	Viséan	*L. nodosa*	1	2.8	-27.0	29.8	n/a	300.7	0.4
Priniodinida	Viséan	*G. bilineatus*	4	2.9	-27.2	30.1	2.70	273.4	10.5
Priniodinida	Tournaisian	*G. typicus*	1	4.2	-26.5	30.7	n/a	640.4	11.7
Priniodinida	Tournaisian	*S. isosticha*	1	4.4	-27.0	31.4	n/a	686.9	12.7
Priniodinida	Tournaisian	*S. quadruplicata / S. crenulata*	13	2.6	-26.8	29.4	1.89	600.5	20.6
Priniodinida	Tournaisian	*S. bransoni / S. wilberti*	1	0.5	-26.1	26.6	n/a	586.0	2.8
Priniodinida	Tournaisian	*S. (E.) sulcata*	1	3.4	-24.8	28.2	n/a	581.0	7.3
Priniodinida	Famennian	*S. (E.) praesulcata*	5	3.0	-25.4	28.4	1.90	689.0	54.7
Priniodinida	Famennian	*P. rhomboidea*	2	-0.2	-26.1	25.9	1.33	829.8	10.3
Priniodinida	Famennian	*P. crepida*	1	-0.9	-24.8	23.9	n/a	872.3	n/a
Priniodinida	Famennian	*P. triangularis*	1	-1.2	-26.3	25.1	n/a	935.4	n/a
Priniodinida	Frasnian	MZ5	1	-1.5	-26.6	25.1	n/a	1060.0	n/a
Ozarkodinida	Serpukhovian	*G. bollandensis*	3	0.5	-27.1	27.6	1.37	340.9	16.9
Ozarkodinida	Serpukhovian	*L. ziegleri*	37	1.4	-26.6	28.0	2.14	288.8	14.3
Ozarkodinida	Viséan	*L. nodosa*	7	1.1	-27.1	28.2	1.35	300.7	0.4
Ozarkodinida	Viséan	*G. bilineatus*	4	3.7	-28.0	31.7	2.45	273.4	10.5
Ozarkodinida	Tournaisian	*G. typicus*	2	3.6	-27.7	31.3	3.75	640.4	11.7
Ozarkodinida	Tournaisian	*S. isosticha*	9	4.5	-27.3	31.8	1.74	686.9	12.7
Ozarkodinida	Tournaisian	*S. quadruplicata / S. crenulata*	49	2.0	-26.2	28.2	2.21	600.5	20.6
Ozarkodinida	Tournaisian	*S. bransoni / S. wilberti*	7	1.8	-27.6	29.4	1.80	586.0	2.8
Ozarkodinida	Tournaisian	*S. (E.) sulcata*	47	2.7	-26.5	29.2	2.00	581.0	7.3
Ozarkodinida	Famennian	*S. (E.) praesulcata*	54	3.3	-27.2	30.5	1.75	689.0	54.7
Ozarkodinida	Famennian	*P. expansa*	6	2.8	-28.0	30.8	2.02	854.7	30.5
Ozarkodinida	Famennian	*P. marginifera*	11	0.2	-27.5	27.7	1.49	806.1	6.1
Ozarkodinida	Famennian	*P. rhomboidea*	7	0.1	-27.4	27.5	2.75	829.8	10.3
Ozarkodinida	Famennian	*P. triangularis*	1	-0.2	-27.9	27.7	n/a	935.4	n/a
Ozarkodinida	Frasnian	MZ6	5	-1.8	-26.5	24.7	1.49	1100.0	n/a
Ozarkodinida	Frasnian	MZ5	6	-0.6	-26.8	26.2	1.43	1060.0	n/a
Ozarkodinida	Frasnian	MZ4	5	-0.9	-25.6	24.7	3.14	1110.0	n/a
Ozarkodinida	Frasnian	MZ1	1	0.1	-26.4	26.5	n/a	1081.0	n/a

Full genus–species names for conodont zones listed in the table: *Gnathodus bollandensis*; *Lochriea ziegleri*; *Lochriea nodosa*; *Gnathodus bilineatus*; *Gnathodus typicus*; *Siphonodella isosticha*; *Siphonodella quadruplicata*; *Siphonodella crenulata*; *Siphonodella bransoni*; *Siphonodella wilberti*; *Siphonodella (Eos.) sulcata*; *Siphonodella (Eos.) praesulcata*; *Palmatolepis rhomboidea*; *Palmatolepis crepida*; *Palmatolepis triangularis*; *Palmatolepis expansa*; *Palmatolepis marginifera*.

standard. The precision of the $\delta^{13}C_{carb}$ value is ±0.04 ‰. All the isotope analyses were made at the Center "Geonauka" of the Institute of Geology of FRC Komi SC UrB RAS (Syktyvkar, Russia). The statistical methods were performed using the PAST 5 software (Hammer *et al.*, 2001).

A preliminary test of the hypothesis was performed on the mean values for conodont zones of $\delta^{13}C_{con}$ and $\delta^{13}C_{carb}$ (data from Zhuravlev, 2023 with additions; Table 1) and the mean most probable CO$_2$ concentrations from the multi-proxy compilation of Foster *et al.*, 2017. Mean values of $\delta^{13}C_{con}$ were calculated separately for ozarkodinid and prioniodinid conodonts. $\delta^{13}C_{con}$ and $\delta^{13}C_{carb}$ data originate from the same samples. All the data derive from the shelf deposits of the northeastern Laurussia (present-day northern Cis-Urals) of Late Devonian – Mississippian age. During this time interval, the region lay within the tropical climate belt of the northern hemisphere (Boucot *et al.*, 2013).

Results

The mean values of the decoupling of C-isotope composition of conodont elements and host carbonates (DELTA C) show a negative correlation with the mean most probable CO$_2$ [atm] in the Late Devonian-Mississippian (Fig. 1). The correlation is weak but significant (R = -0.538, n = 32, p = 0.0015).

Taking into account some taxonomic differences in $\delta^{13}C_{con}$ (Zhuravlev, 2023), it is reasonable to assume that the relationship between DELTA C and CO$_2$ [atm] is taxon-specific, at least at high taxonomic levels.

Representatives of the orders Ozarkodinida and Prioniodinida exhibit similar but not identical correlations between DELTA C and CO$_2$ [atm] (R = -0.548, n = 18, p = 0.0019 and R = -0.607, n = 14, p = 0.0213, respectively). Ordinary least squares regressions reveal nearly equal gradients (-71.6 and -66.2) but different intercepts (2744.6 for Ozarkodinida and 2465.7 for Prioniodinida) (Fig. 1).

Discussion

The present study material is palaeogeographically constrained, representing a tropical epicontinental basin within northeastern Laurussia. The anticipated low seasonal and spatial variability in pCO$_2$ [atm] characteristic of tropical environments (Cheng *et al.*, 2022) suggests the potential for this dataset to be correlated with global mean CO$_2$ [atm] estimates. However, robust validation of this hypothesis necessitates evaluation using a broader stratigraphic record encompassing diverse palaeoenvironment and climatic

conditions. Localities exhibiting both shallow marine carbonates containing conodonts and associated pedogenic carbonates (e.g. the Viséan-Serpukhovian interval within the central East European Platform) represent particularly promising sites for testing the proposed correlation utilizing multiple CO_2 [atm] proxies.

Acknowledging the complex relationship between C-isotope composition of phytoplankton and CO_2 [atm], which varies significantly across different environments and algal groups (Popp *et al.*, 1999), a taxonomic approach to conodont analysis is warranted. It is hypothesized that the correlation between DELTA C and CO_2 [atm] may exhibit substantial variation among conodont taxa or ecological groupings reflecting differing trophic strategies and phytoplankton consumption patterns. Preliminary findings from Ozarkodinida and Prioniodinida suggest a shared dependence mechanism, as indicated by similar DELTA C – CO_2 [atm] regression gradients; however, divergent intercepts likely reflect variations in vital effects or differences in habitat preference and foraging behaviour among these taxa. Further refinement of our understanding regarding the trophic ecology of conodont taxa is crucial to mitigating potential taxonomical effects on DELTA C values.

Possible implications of the proposed hypothesis include reconstruction of spatial variations in CO_2 concentration in atmosphere in the Palaeozoic (e.g. due to emissions of CO_2 induced by large igneous provinces) and identification of regional CO_2 dynamics in relation to the climate changes. These preliminary results allow the hypothesis to be formulated that the decoupling of the C-isotope composition of conodont elements and host carbonates (DELTA C) can be used as a proxy for the CO_2 content in the ancient atmosphere.

Data availability

The data used in this study are available in Kotik *et al.*, (2021) and in the supplementary materials to Zhuravlev (2023).

Acknowledgements

Author contributions

Conceptualization AVZ; Data curation AVZ; Formal analysis AVZ; Investigation AVZ; Writing – original draft AVZ.

Competing interests

The author declares no conflicts of interests.

Ethics and AI use

Artificial intelligence powered by a large language model was used to proof-reading the manuscript.

Funding

References

Balter, V., Martin, J.E., Tacail, T., Suan, G., Renaud, S. and Girard, C. 2019. Calcium stable isotopes place Devonian conodonts as first level consumers. *Geochemical Perspectives Letters* 10, 36–39. https://doi.org/10.7185/geochemlet.1912.

Beerling, D.J., McElwain, J.C. and Osborne, C.P. 1998. Stomatal responses of the 'living fossil' *Ginkgo biloba* L. to changes in atmospheric CO_2 concentrations. *Journal of Experimental Botany* 49:326, 1603–1607. https://doi.org/10.1093/jxb/49.326.1603.

Berner, R.A. 1994. GEOCARB II; a revised model of atmospheric CO_2 over Phanerozoic time. *American Journal of Science* 294:1, 56–91. https://doi.org/10.2475/ajs.294.1.56.

Berner, R.A. and Kothavala, Z. 2001. GEOCARB III: A revised model of atmospheric CO_2 over Phanerozoic time. *American Journal of Science* 301:2, 182–204. https://doi.org/10.2475/ajs.301.2.182.

Boucot, A.J., Chen, X. and Scotese, C.R. 2013. *Phanerozoic Paleoclimate: An Atlas of Lithologic Indicators of Climate.* SEPM (Society for Sedimentary Geology), Concepts in Sedimentology and Paleontology, no. 11. 478 pp. ISBN 978-1-56576-282-4.

Breecker, D.O., Sharp, Z.D. and McFadden, L.D. 2010. Atmospheric CO_2 concentrations during ancient greenhouse climates were similar to those predicted for A.D. 2100. *Proceedings of the National Academy of Sciences USA* 107:2, 576–580. https://doi.org/10.1073/pnas.0902323106.

Came, R.E., Eiler, J.M., Veizer, J., Azmy, K., Brand, U. and Weidman, C.R. 2007. Coupling of surface temperatures and atmospheric CO_2 concentrations during the Palaeozoic era. *Nature* 449:7159, 198–201. https://doi.org/10.1038/nature06085.

Cheng, W., Dan, L., Deng, X., Feng, J., Wang, Y., Peng, J., Tian, J., Qi, W., Liu, Z., Zheng, X., Zhou, D., Jiang, S., Zhao, H. and Wang, X. 2022. Global monthly gridded atmospheric carbon dioxide concentrations under the historical and future scenarios. *Scientific Data* 9, 83. https://doi.org/10.1038/s41597-022-01196-7.

Crowley, J.K. and Berner, R.A. 2001. CO_2 and climate change. *Science* 292, 870–872. https://doi.org/10.1126/science.1061664.

Ekart, D.D., Cerling, T.E., Montañez, I.P. and Tabor, N.J. 1999. A 400 million year carbon isotope record of pedogenic carbonate: implications for paleoatmospheric carbon dioxide. *American Journal of Science* 299, 805–827.

Fielding, C.R., Frank, T.D. and Isbell, J.L. 2008. The late Paleozoic ice age—A review of current understanding and synthesis of global climate patterns. In: Fielding, C.R., Frank, T.D. and Isbell, J.L. (Eds.). *Resolving the Late Paleozoic Ice Age in Time and Space.* Geological Society of America, 343–354. https://doi.org/10.1130/2008.2441(24).

Foote, E.N. 1856. Circumstances affecting the heat of Sun's rays. *American Journal of Science and Arts* XXII(LXVI), 382–383.

Foster, G., Royer, D. and Lunt, D. 2017. Future climate forcing potentially without precedent in the last 420 million years. *Nature Communications* 8, 14845. https://doi.org/10.1038/ncomms14845.

Freeman, K.H. and Hayes, J.M. 1992. Fractionation of carbon isotopes by phytoplankton and estimates of ancient CO_2 levels. *Global Biogeochemical Cycles* 6, 185–198.

Goddéris, Y., Donnadieu, Y., Le Hir, G., Lefebvre, V. and Nardin, E. 2014. The role of paleogeography in the Phanerozoic history of atmospheric CO_2 and climate. *Earth-Science Reviews* 128, 122–138. https://doi.org/10.1016/j.earscirev.2013.11.004.

Grossman, E.L. and Joachimski, M.M. 2022. Ocean temperatures through the Phanerozoic reassessed. *Scientific Reports* 12, 8938. https://doi.org/10.1038/s41598-022-11493-1.

Hammer, Ø., Harper, D.A.T. and Ryan, P.D. 2001. PAST: Paleontological statistics software package for education and data analysis. *Palaeontologia Electronica* 4:1, 1–9.

Haq, B.U. and Schutter, S.R. 2008. A chronology of Paleozoic sea-level changes. *Science* 322, 64–68. https://doi.org/10.1126/science.1161648.

Harris, A.G. and Sweet, W.C. 1989. Mechanical and chemical techniques for separating microfossils from rock. In: Feldmann, R.M., Chapman, R.E. and Hannibal, J.T. (eds). *Paleotechniques*. Paleontological Society Special Publication 4, 70–86.

Hartke, E.R., Bradley, D., Cramer, B.D., Calner, M., Melchin, M.J., Barnett, B.A., Oborny, S.C. and Bancroft, A.M. 2021. Decoupling $\delta^{13}C_{carb}$ and $\delta^{13}C_{org}$ at the onset of the Ireviken Carbon Isotope Excursion: $\Delta^{13}C$ and organic carbon burial (f_{org}) during a Silurian oceanic anoxic event. *Global and Planetary Change* 196, 103373. https://doi.org/10.1016/j.gloplacha.2020.103373.

Hayes, J.M., Strauss, H. and Kaufman, A.J. 1999. The abundance of ^{13}C in marine organic matter and isotopic fractionation in the global biogeochemical cycle of carbon during the past 800 Ma. *Chemical Geology* 161, 103–125.

Kotik, I.S., Zhuravlev, A.V., Maydl, T.V., Bushnev, D.A. and Smoleva, I.V. 2021. Early–Middle Frasnian (Late Devonian) carbon isotope event in the Timan–Pechora Basin (Chernyshev Swell, Pymvashor River section, North Cis-Urals, Russia). *Geologica Acta* 19:3, 1–17. https://doi.org/10.1344/GeologicaActa2021.19.3.

Lenton, T.M., Daines, S.J. and Mills, B.J.W. 2018. COPSE reloaded: An improved model of biogeochemical cycling over Phanerozoic time. *Earth-Science Reviews* 178, 1–28. https://doi.org/10.1016/j.earscirev.2017.12.004.

Marcilly, C.M., Torsvik, T.H., Domeier, M. and Royer, D.L. 2021. New paleogeographic and degassing parameters for long-term carbon cycle models. *Gondwana Research* 97, 176–203. https://doi.org/10.1016/j.gr.2021.05.016.

McKenzie, N.R. and Jiang, H. 2019. Earth's outgassing and climatic transitions: The slow burn towards environmental catastrophes? *Elements* 15:5, 325–330. https://doi.org/10.2138/gselements.15.5.325.

Mills, B.J.W., Krause, A.J., Scotese, C.R., Hill, D.J., Shields, G.A. and Lenton, T.M. 2019. Modelling the long-term carbon cycle, atmospheric CO_2, and Earth surface temperature from late Neoproterozoic to present day. *Gondwana Research* 67, 172–186. https://doi.org/10.1016/j.gr.2018.12.001

Montañez, I.P. and Poulsen, C.J. 2013. The Late Paleozoic Ice Age: an evolving paradigm. *Annual Review of Earth and Planetary Sciences* 41, 24.1–24.28. https://doi.org/10.1146/annurev.earth.031208.100118.

Mora, C.I., Driese, S.G. and Colarusso, L.A. 1996. Middle and Late Paleozoic atmospheric CO_2 levels from soil carbonate and organic matter. *Science* 271, 1105–1107.

Muchez, P., Peeters, C., Keppens, E. and Viaene, W.A. 1993. Stable isotopic composition of paleosols in the Lower Viséan of eastern Belgium: evidence of evaporation and soil-gas CO_2. *Chemical Geology* 106, 389–396.

Pagani, M., Arthur, M.A. and Freeman, K.H. 1999a. Miocene evolution of atmospheric carbon dioxide. *Paleoceanography* 14, 273–292.

Pagani, M., Freeman, K.H. and Arthur, M.A. 1999b. Late Miocene atmospheric CO_2 concentrations and the expansion of C_4 grasses. *Science* 285, 876–879.

Percival, L.M.E., Matsumoto, H., Callegaro, S., Erba, E., Kerr, A.C., Mutterlose, J. and Suzuki, K. 2024. Cretaceous large igneous provinces: from volcanic formation to environmental catastrophes and biological crises. *Geological Society Special Publications* 544:1, sp544-2023-88. https://doi.org/10.1144/SP544-2023-88.

Popp, B.N., Hanson, K.L., Dore, J.E., Bidigare, R.R., Laws, E.A. and Wakeham, S.G. 1999. Controls on the carbon isotopic composition of phytoplankton. In: Abrantes, F. and Mix, A.C. (Eds.), *Reconstructing Ocean History*. Springer, Boston, MA. https://doi.org/10.1007/978-1-4615-4197-4_21.

Royer, D.L. 2001. Stomatal density and stomatal index as indicators of paleoatmospheric CO_2 concentration. *Review of Palaeobotany and Palynology* 114:1–2, 1–28. https://doi.org/10.1016/S0034-6667(00)00074-9.

Royer, D.L., Berner, R.A., Montañez, I.P., Tabor, N.J. and Beerling, D.J. 2004. CO_2 as a primary driver of Phanerozoic climate. *GSA Today* 14, 4–10. https://doi.org/10.1130/1052-5173(2004)014¡4CAAPDO¿2.0.CO;2.

Royer, D.L., Donnadieu, Y., Park, J., Kowalczyk, J. and Goddéris, Y. 2014. Error analysis of CO_2 and O_2 estimates from the long-term geochemical model GEOCARBSULF. *American Journal of Science* 314:9, 1259–1283.

Torsvik, T.H., Royer, D.L., Marcilly, C.M. and Werner, S.C. 2024. User-friendly carbon-cycle modelling and aspects of Phanerozoic climate change. *Applied Computing and Geosciences* 23, 100180. https://doi.org/10.1016/j.acags.2024.100180.

Veizer, J. and Prokoph, A. 2015. Temperatures and oxygen isotopic composition of Phanerozoic oceans. *Earth-Science Reviews* 146, 92–104. https://doi.org/10.1016/j.earscirev.2015.03.008.

Witkowski, C.R., Weijers, J.W.H., Blais, B., Schouten, S. and Sinninghe Damsté, J.S. 2018. Molecular fossils from phytoplankton reveal secular pCO_2 trend over the Phanerozoic. *Science Advances* 4(11), eaat4556. https://doi.org/10.1126/sciadv.aat4556.

Wolf-Gladrow, D.A., Riebesell, U., Burkhardt, S. and Bijma, J. 1999. Direct effects of CO_2 on growth and isotopic composition of marine plankton. *Tellus B* 51, 461–476.

Yoshioka, T. 1997. Phytoplanktonic carbon isotope fractionation: equations accounting for CO_2-concentrating mechanisms. *Journal of Plankton Research* 19:10, 1455–1476.

Zhuravlev, A.V. 2020. Trophic position of some Late Devonian–Carboniferous (Mississippian) conodonts revealed on carbon organic matter isotope signatures: a case study of the East European basin. *Geodiversitas* 42:24, 443–453. https://doi.org/10.5252/geodiversitas2020v42a24.

Zhuravlev, A.V. 2023. Carbon isotope study of conodont elements: Applications and limitations. *Marine Micropaleontology* 178, 102200. https://doi.org/10.1016/j.marmicro.2022.102200.